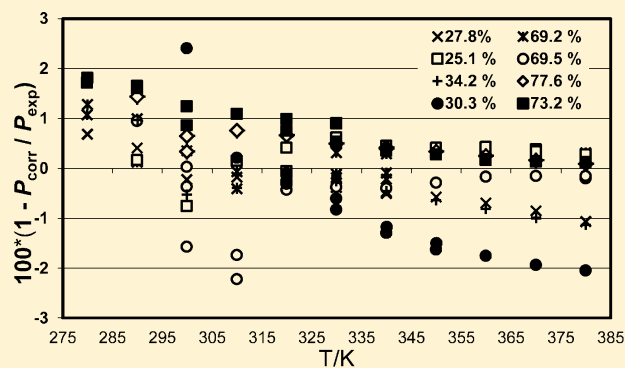


Bubble-Point Measurements of Eight Binary Mixtures for Organic Rankine Cycle Applications

Stephanie L. Outcalt* and Eric W. Lemmon

Material Measurement Laboratory, Applied Chemicals and Materials Division, National Institute of Standards and Technology, 325 Broadway, Boulder, Colorado 80305-3337, United States

ABSTRACT: The bubble-point pressures of two compositions of each of eight binary mixtures have been measured over a temperature range of 270 K to 380 K. Six of the mixtures included pentane, which was mixed with 1,1,1,3,3-pentafluoropropane (R-245fa); methyl perfluoropropyl ether (R-E347mcc); 1,1,1,2,2,4,5,5,5-nonafluoro-4-(trifluoromethyl)-3-pentanone; 1,1-dichloro-1-fluoroethane (R-141b); *trans*-1,3,3,3-tetrafluoropropene (R-1234ze(E)); and dimethyl ether. The two remaining binary mixtures were 1,1,1,2,2,4,5,5,5-nonafluoro-4-(trifluoromethyl)-3-pentanone + methyl perfluoropropyl ether (R-E347mcc) and butane + R-245fa. Interaction parameters for a Helmholtz energy mixture model were fitted for each mixture. Bubble-point data are reported as well as mixture model parameters, along with deviations of the data from their respective equations. These mixtures are of interest as working fluids in organic Rankine power cycles.



1. INTRODUCTION

The work presented here was undertaken in response to a search for working fluids, especially environmentally friendly fluids, which could be used in power production from low to medium temperature heat sources in organic Rankine cycle (ORC) technology. With the exception that it employs an organic working fluid instead of water, the ORC cycle is essentially the same as the conventional Clausius–Rankine steam-based cycle. Compared to water, the volume ratio of organic fluids is typically orders of magnitude smaller. A major advantage of smaller volume ratios is the reduced complexity and smaller cost of expansion devices (turbines) used in power generation cycles.¹

ORC systems that use pure component working fluids may suffer sizable loss of efficiency as the result of two primary reasons:² (1) In most applications the temperatures of the heat sink and the source fluid vary during the heat transfer process, while the temperature of the working fluid during evaporation and condensation is a constant. This may cause a pinch point in the evaporator and condenser and result in large temperature differences at one end of the heat exchanger. This leads to process irreversibility and thus lower efficiency. (2) The thermodynamic properties of a pure working fluid may not be well matched to the requirements imposed by the Rankine cycle and the desired application. In contrast, a working fluid mixture (with the appropriate temperature glide) may provide a good match to the temperature profiles of the condenser and evaporator and thus lead to increased efficiency of the system.

In the present study, bubble-point pressures of binary mixtures of working fluids were measured. The data reported here provide information to aid in the investigation of the

viability of these mixtures as working fluids that have potential to increase efficiency and cost savings in energy production. The mixtures studied were chosen with the goal of creating an organic working fluid with optimal thermodynamic properties as well as a lower global warming potential (GWP) than those of existing working fluids. Mixing two fluids can take advantage of the positive characteristics of each individual component while mitigating those that are undesirable.

2. MIXTURE PREPARATION

The mixtures measured in this work were prepared gravimetrically. The pure fluids included in each mixture were obtained from commercial sources. The stated manufacturer purities were as follows: 1,1,1,3,3-pentafluoropropane (CAS No. 460-73-1, hereafter referred to as R-245fa) 98.8 %; methyl perfluoropropyl ether (CAS No. 375-03-1, R-E347mcc) 99.5 %; 1,1,1,2,2,4,5,5,5-nonafluoro-4-(trifluoromethyl)-3-pentanone (CAS No. 756-13-8, Novec 649) 99.9 %; 1,1-dichloro-1-fluoroethane (CAS No. 1717-00-6, R-141b) 99.8 %; *trans*-1,3,3,3-tetrafluoropropene (CAS No. 29118-24-9, R-1234ze(E)) 99.993 %; dimethyl ether (CAS No. 115-10-6) 99.9 %; butane (CAS No. 106-97-8) 99.9 %; and pentane (CAS No. 109-66-0) 99 %. Analyses of the pure fluids R-245fa, R-E347mcc, Novec 649, R-141b, and pentane were performed in our laboratory by gas chromatography–mass spectrometry (GC-MS). [Here, to describe materials and experimental

Received: March 14, 2013

Accepted: May 3, 2013

Published: May 24, 2013

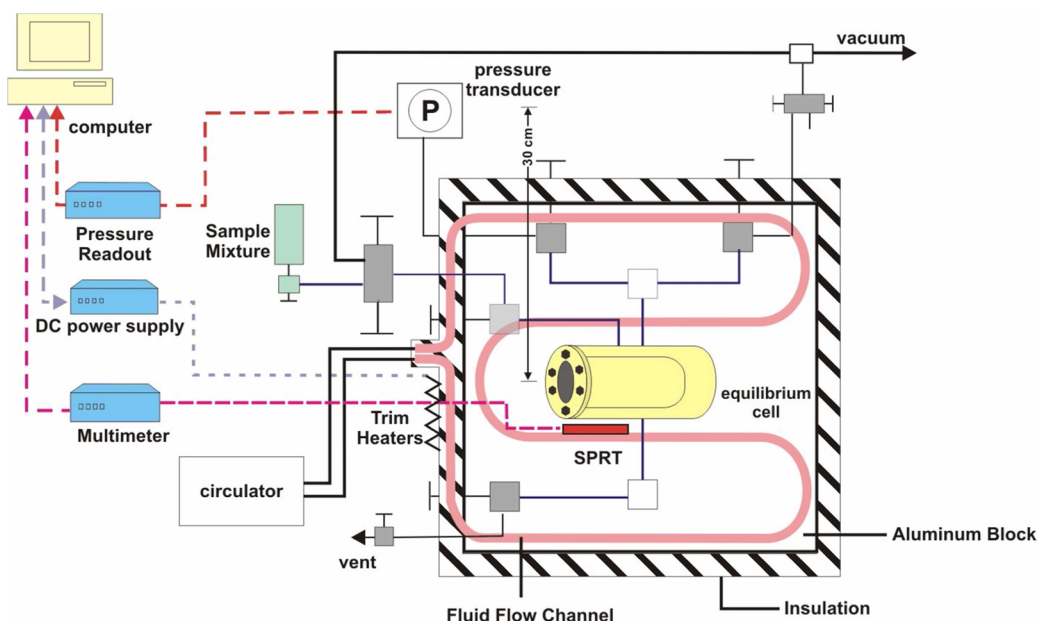


Figure 1. Schematic of the apparatus used to make the bubble-point measurements.

procedures adequately, it is occasionally necessary to identify commercial products by manufacturers' names or labels. In no instance does such identification imply endorsement by the National Institute of Standards and Technology, nor does it imply that the particular product or equipment is necessarily the best available for the purpose.] Spectral peaks were interpreted with guidance from the NIST/EPA/NIH Mass Spectral Database³ and the CRC Handbook of Basic Tables for Chemical Analysis.⁴ These analyses indicated that these samples were within the manufacturer's specifications. All of the samples were used without further purification.

Mixtures were prepared in sealed 300 mL stainless steel cylinders. The fluid with the higher boiling point was added first, then the second component. The vapor space above the mixture samples was degassed by freezing the sample with liquid nitrogen and opening the cylinder to vacuum. After evacuation, the sample was then heated (in the closed stainless steel cylinder) to drive the greatest possible amount of the remaining volatile impurities into the vapor space. The entire cycle (freezing, evacuation, and heating) was repeated a minimum of three times for each sample. In the instances where one or both of the components had boiling points below room temperature, this procedure was followed after the addition of the first component as well as upon completion of the mixture. Mixtures were prepared with the goal of filling the sample cylinder to between 260 mL and the maximum volume of 300 mL at the target composition, at ambient temperature. Thus, in each completed mixture cylinder there was a space above the liquid phase. In mixtures where both components had boiling points above ambient temperature, this space was of course evacuated.

A balance with a precision of 0.1 mg was used in the preparation of the mixtures. Utilizing the double-substitution weighing design of Harris and Torres,⁵ measurement of the mass of each component consisted of weighing four masses: (1) a reference cylinder of approximately the same mass and volume as the empty sample cylinder, (2) the sample cylinder, (3) the sample cylinder plus a 20 g sensitivity weight, and (4) the reference cylinder plus the 20 g sensitivity weight. This

weighing sequence was repeated four times for each mass determination. The density of ambient air was calculated based on measurements of temperature, pressure, and relative humidity, and the weighings were corrected for the effects of air buoyancy. The standard deviation of the repeat weighings was at most 1.5 mg. The uncertainty of the measured mixture composition will be discussed in detail in a later section.

3. EXPERIMENTAL SECTION

A schematic of the instrument used to make the measurements is shown in Figure 1. Details of the instrument are given in Outcalt and Lee,⁶ thus only a brief description will be provided here. The heart of the instrument was a cylindrical stainless steel cell with a sapphire window on each end so that the liquid level in the cell was visible. The cell had a volume of approximately 30 mL. The cell and all of the system valves were housed inside a temperature-controlled, insulated aluminum block. The operating range of the apparatus was 270 K to 380 K, to pressures of 6 MPa. To make the bubble-point measurements reported herein, the instrument was modified slightly from that described in Outcalt and Lee.⁶ The pump used to circulate the sample under test, as well as the associated plumbing, was removed. This modification decreased the system volume slightly, but more importantly removed a portion of the system volume that was outside the thermostatted block, thus eliminating a source of thermal gradients from the system.

In an effort to load the liquid phase of the mixture sample, the sample bottle was connected to the system in an inverted position. Prior to loading a sample into the system, the system was evacuated and then cooled to approximately 270 K, and the pressure reading under vacuum was recorded. Reported pressures have been adjusted to reflect any offset of the pressure transducer from zero. The sample was then quickly loaded into the system until only a small vapor space remained in the equilibrium cell.

Assumptions that are made in this method of measuring the bubble point of the mixtures are: (1) the liquid composition in the cell is equal to the bulk composition of the mixture in the

sample bottle, and (2) by loading the cell almost full of liquid (only a very small vapor space remaining), the composition of the liquid that has been loaded into the system is nearly equal to that of the sample bottle mixture, and thus the pressure of the vapor phase is the bubble-point pressure of that composition at a given temperature. Following these assumptions, bubble-point pressures of each of the mixtures listed in Tables 1 to 8 were measured at temperatures ranging

Table 1. Measured Bubble-Point Pressures for the System R-245fa (1) + Butane (2) at Temperature T , Pressure P , and Liquid Mole Fraction x^a

$x_1 = 0.278 \pm 0.003$				
T/K	P/kPa	$u(P)/kPa$	$(u(P)/P) \cdot 100$	$(1 - P_{EOS}/P_{exp}) \cdot 100$
280.00	169.00	5.28	3.13	0.68
290.00	237.84	5.46	2.30	0.41
300.00	325.02	5.64	1.74	-0.23
310.00	437.11	5.83	1.33	-0.18
320.00	575.17	7.46	1.30	-0.28
330.00	743.89	7.64	1.03	-0.29
330.00	743.19	7.63	1.03	-0.39
340.00	945.18	7.90	0.84	-0.48
340.00	944.90	7.90	0.84	-0.51
350.00	1184.87	8.21	0.69	-0.58
360.00	1466.18	8.56	0.58	-0.70
370.00	1793.14	9.03	0.50	-0.86
380.00	2170.37	9.53	0.44	-1.07
$x_1 = 0.692 \pm 0.006$				
T/K	P/kPa	$u(P)/kPa$	$(u(P)/P) \cdot 100$	$(1 - P_{EOS}/P_{exp}) \cdot 100$
279.95	162.77	6.47	3.97	1.07
280.02	163.50	6.47	3.96	1.28
290.00	227.74	6.57	2.88	0.99
290.00	225.74	6.57	2.91	0.12
300.00	309.17	6.68	2.16	0.35
310.00	410.79	6.79	1.65	-0.41
310.00	412.18	6.79	1.65	-0.07
320.00	541.11	9.29	1.72	-0.19
320.00	540.78	9.29	1.72	-0.25
330.00	703.00	9.38	1.33	0.31
330.00	699.50	9.38	1.34	-0.19
330.00	699.99	9.38	1.34	-0.12
340.00	895.03	9.55	1.07	0.29
340.00	891.58	9.55	1.07	-0.10
340.00	890.49	9.55	1.07	-0.22
350.00	1125.39	9.74	0.87	0.36
360.00	1396.30	10.03	0.72	0.32
370.00	1714.70	10.34	0.60	0.34
370.00	1714.82	10.34	0.60	0.34
380.00	2084.40	10.77	0.52	0.31

^aStandard uncertainties u are $u(T) = 0.03$ K. The values of $u(x_1)$ and $u(P)$ are given in the table.

from 270 K to 380 K in 10 K increments. As the temperature was increased, the liquid expanded, eventually filling the cell with compressed liquid. As a result it was necessary to periodically release a small amount of liquid from the bottom of the cell to maintain a vapor space. Repeat measurements were conducted at a minimum of two temperatures. These repeats established the repeatability of the measurements and also helped to determine whether the loss of small amounts of the liquid phase affected the sample composition to the extent that

Table 2. Measured Bubble-Point Pressures for the System R-141b (1) + Pentane (2) at Temperature T , Pressure P , and Liquid Mole Fraction x^a

$x_1 = 0.251 \pm 0.020$				
T/K	P/kPa	$u(P)/kPa$	$(u(P)/P) \cdot 100$	$(1 - P_{EOS}/P_{exp}) \cdot 100$
290.00	57.38	1.96	3.42	0.16
300.00	82.76	1.98	2.39	-0.76
310.00	118.19	2.00	1.69	0.15
320.00	163.60	4.82	2.95	0.40
320.00	162.84	4.82	2.96	-0.06
330.00	221.38	4.83	2.18	0.61
340.00	292.55	4.85	1.66	0.44
350.00	380.29	4.86	1.28	0.40
360.00	486.56	4.89	1.00	0.39
360.00	486.72	4.89	1.00	0.42
370.00	613.64	4.91	0.80	0.37
370.00	613.39	4.91	0.80	0.33
380.00	763.21	4.98	0.65	0.27
$x_1 = 0.695 \pm 0.022$				
T/K	P/kPa	$u(P)/kPa$	$(u(P)/P) \cdot 100$	$(1 - P_{EOS}/P_{exp}) \cdot 100$
289.99	61.34	2.38	3.88	0.94
300.00	87.13	2.39	2.75	-1.57
300.00	88.52	2.39	2.70	0.02
300.00	88.17	2.39	2.71	-0.37
310.00	123.13	2.41	1.96	-1.74
310.00	122.56	2.41	1.97	-2.22
320.00	172.55	6.41	3.71	-0.25
320.00	172.24	6.41	3.72	-0.44
330.00	232.72	6.42	2.76	-0.38
340.00	307.98	6.42	2.09	-0.40
350.00	400.91	6.43	1.60	-0.29
360.00	513.55	6.44	1.25	-0.17
370.00	647.72	6.44	0.99	-0.16
380.00	805.84	6.50	0.81	-0.20
380.00	806.22	6.50	0.81	-0.16

^aStandard uncertainties u are $u(T) = 0.03$ K. The values of $u(x_1)$ and $u(P)$ are given in the table.

duplicate measurements at a given temperature yielded different bubble-point pressures. In almost all instances this was not the case.

4. UNCERTAINTY ANALYSIS

The expanded uncertainty for our bubble-point measurements was calculated by the root-sum-of-squares method,⁷ taking into account five principle sources of uncertainty: temperature, pressure, sample composition, measurement repeatability, and head pressure correction. The standard platinum resistance thermometer (SPRT) and the pressure transducer used for our measurements were calibrated regularly. The calibration of the SPRT was checked against the triple points of mercury and water and the freezing point of indium. The standard combined uncertainty in our temperature measurements including the uncertainties in the SPRT, the multimeter used to read it, the calibration, and the possible temperature gradient between the equilibrium cell and the SPRT is estimated to be 30 mK.

The quartz-crystal pressure transducer (PT) was calibrated with a NIST-traceable piston gauge. The manufacturer's stated uncertainty of the PT is 0.01 % of full range, or 0.7 kPa. As documented in Outcalt and Lee,⁶ tests with ultrahigh-purity propane in the saturated state yielded deviations from the

Table 3. Measured Bubble-Point Pressures for the System R-245fa (1) + Pentane (2) at Temperature T , Pressure P , and Liquid Mole Fraction x^a

$x_1 = 0.342 \pm 0.006$				
T/K	P/kPa	$u(P)/kPa$	$(u(P)/P) \cdot 100$	$(1 - P_{EOS}/P_{exp}) \cdot 100$
290.06	129.71	3.02	2.33	0.97
300.00	180.22	3.10	1.72	-0.53
310.00	248.46	3.19	1.29	-0.39
320.00	335.25	5.80	1.73	-0.09
330.00	441.45	5.86	1.33	-0.16
330.00	441.00	5.86	1.33	-0.26
340.00	569.25	5.93	1.04	-0.46
350.00	722.89	6.01	0.83	-0.64
360.00	904.42	6.18	0.68	-0.81
370.00	1116.46	6.41	0.57	-0.99
370.00	1116.30	6.41	0.57	-1.00
380.00	1361.73	6.69	0.49	-1.14
$x_1 = 0.776 \pm 0.009$				
T/K	P/kPa	$u(P)/kPa$	$(u(P)/P) \cdot 100$	$(1 - P_{EOS}/P_{exp}) \cdot 100$
290.02	133.17	2.78	2.09	1.44
300.00	188.67	2.86	1.52	0.33
300.00	189.26	2.86	1.51	0.64
310.00	264.53	2.94	1.11	0.76
320.00	360.29	7.23	2.01	0.66
330.00	480.12	7.28	1.52	0.49
340.00	628.40	7.33	1.17	0.42
340.00	628.26	7.33	1.17	0.39
350.00	808.67	7.43	0.92	0.33
360.00	1025.10	7.60	0.74	0.24
370.00	1282.01	7.82	0.61	0.16
380.00	1584.70	8.15	0.51	0.09

^aStandard uncertainties u are $u(T) = 0.03$ K. The values of $u(x_1)$ and $u(P)$ are given in the table.

equation of state of Lemmon et al.⁸ for a vapor pressure of no greater than 0.08 % of the measured pressure in the temperature range of the measurements reported here. At higher measured pressures, this number is greater than the 0.7 kPa estimated by the manufacturer. Thus, as a conservative estimate of the pressure uncertainty, the greater of 0.7 kPa or 0.1 % has been used in the calculation of the overall combined uncertainty of the bubble-point pressures reported here.

The uncertainty in the composition of the mixture is by far the most difficult to estimate accurately. Numerous variables such as sample purity, uncertainty in the weighings during sample preparation, and the transfer of the mixture sample into the measuring system will affect the composition of the fluid mixture that was ultimately measured. In terms of sample preparation, there is negligible uncertainty in the weighings. To account for the possibility that the degassing of the samples was not complete, a calculation was done assuming that air represented a 0.001 mole fraction impurity in each of the mixtures. Nitrogen was used to represent air in the calculations. As there are no data to represent the solubility of air in these mixtures, the partial pressure of nitrogen was used to represent the impurity. An estimate of the composition of the liquid that was transferred to the cell during the loading process was done by calculating the composition of the liquid phase in the sample bottle at ambient temperature (298 K). The equations described in the Results and Correlation of Data section were used to calculate the compositions of the liquid and vapor

Table 4. Measured Bubble-Point Pressures for the System R-1234ze(E) (1) + Pentane (2) at Temperature T , Pressure P , and Liquid Mole Fraction x^a

$x_1 = 0.303 \pm 0.007$				
T/K	P/kPa	$u(P)/kPa$	$(u(P)/P) \cdot 100$	$(1 - P_{EOS}/P_{exp}) \cdot 100$
270.00	132.65	5.26	7.94	3.86
279.95	181.57	5.88	6.47	1.71
290.00	248.03	6.85	5.53	1.60
300.00	333.56	8.27	4.96	2.40
310.00	426.25	10.20	4.79	0.21
320.00	543.88	13.40	4.93	-0.31
320.00	545.02	13.40	4.92	-0.10
330.00	682.61	16.30	4.77	-0.83
330.00	684.14	16.30	4.76	-0.61
340.07	846.77	19.89	4.70	-1.18
340.00	844.56	19.87	4.70	-1.30
350.07	1035.01	24.21	4.68	-1.51
350.00	1032.23	24.03	4.66	-1.63
360.00	1248.92	28.90	4.63	-1.76
370.00	1493.52	34.40	4.61	-1.94
380.00	1768.90	40.54	4.58	-2.05
$x_1 = 0.732 \pm 0.008$				
T/K	P/kPa	$u(P)/kPa$	$(u(P)/P) \cdot 100$	$(1 - P_{EOS}/P_{exp}) \cdot 100$
269.90	169.92	5.25	3.09	-1.46
270.01	170.91	5.25	3.07	-1.63
279.92	243.14	5.32	2.19	-1.30
279.99	243.95	5.32	2.18	-1.40
290.00	338.88	5.44	1.60	-1.16
290.00	339.05	5.44	1.60	-1.21
300.00	456.49	5.61	1.23	-0.37
300.00	458.26	5.61	1.22	-0.75
310.00	607.58	5.86	0.96	-0.58
320.00	788.44	8.46	1.07	-0.20
320.00	790.34	8.46	1.07	-0.45
330.00	1006.75	9.06	0.90	0.05
330.00	1010.53	9.07	0.90	-0.32
330.00	1010.61	9.07	0.90	-0.33
340.00	1266.57	9.76	0.77	0.24
350.00	1572.69	10.89	0.69	0.35
350.00	1572.67	10.89	0.69	0.35
360.00	1927.75	12.37	0.64	0.49
360.00	1927.97	12.37	0.64	0.48
370.00	2337.92	14.41	0.62	0.56
380.00	2805.99	17.30	0.62	0.62

^aStandard uncertainties u are $u(T) = 0.03$ K. The values of $u(x_1)$ and $u(P)$ are given in the table.

phases by considering the reported composition of each sample as the bulk composition and the bulk density to be the total number of grams of material added to the 300 mL stainless steel sample cylinder for each mixture. The difference between the predicted pressure at the reported bulk composition and the pressure at the calculated liquid composition was considered to be the uncertainty in the composition due to the loading procedure. This uncertainty was negligible for all of the mixtures except the R1234ze(E) + pentane.

The repeatability of our bubble-point measurements was determined by repeating measurements at a minimum of two temperatures for each sample studied. The standard deviation was then taken as the repeatability. To be conservative in our uncertainty estimates, the largest of the standard deviation

Table 5. Measured Bubble-Point Pressures for the System DME (1) + Pentane (2) at Temperature T , Pressure P , and Liquid Mole Fraction x^a

$x_1 = 0.392 \pm 0.006$				
T/K	P/kPa	$u(P)/kPa$	$(u(P)/P) \cdot 100$	$(1 - P_{EOS}/P_{exp}) \cdot 100$
280.00	185.74	5.94	3.20	5.84
280.00	183.26	5.94	3.24	4.75
290.03	241.48	6.10	2.52	1.08
300.00	323.15	6.26	1.94	1.52
310.00	425.98	6.43	1.51	2.40
310.00	423.02	6.43	1.52	1.72
320.00	541.47	7.57	1.40	1.51
320.00	541.88	7.57	1.40	1.58
330.00	663.68	7.74	1.17	-1.40
330.00	663.95	7.74	1.17	-1.36
340.00	826.04	7.96	0.96	-1.31
340.00	826.75	7.96	0.96	-1.22
340.00	823.98	7.96	0.97	-1.56
350.00	1013.92	8.22	0.81	-1.27
360.00	1234.82	8.56	0.69	-0.82
360.00	1233.31	8.56	0.69	-0.94
370.00	1482.58	8.89	0.60	-0.68
380.00	1765.56	9.28	0.53	-0.36
380.00	1764.50	9.28	0.53	-0.42
$x_1 = 0.679 \pm 0.006$				
T/K	P/kPa	$u(P)/kPa$	$(u(P)/P) \cdot 100$	$(1 - P_{EOS}/P_{exp}) \cdot 100$
269.99	187.00	6.17	3.30	-1.50
280.00	264.04	6.32	2.39	-0.81
290.00	362.14	6.47	1.79	-0.38
300.00	489.02	6.63	1.36	0.83
310.00	630.24	6.80	1.08	-0.57
310.00	633.10	6.80	1.07	-0.11
310.00	633.53	6.80	1.07	-0.05
320.00	811.02	7.95	0.98	-0.27
320.00	810.47	7.95	0.98	-0.34
330.00	1026.36	8.21	0.80	0.00
340.00	1280.28	8.56	0.67	0.30
350.00	1576.05	8.88	0.56	0.61
360.00	1916.41	9.35	0.49	0.91
370.00	2306.60	9.86	0.43	1.28
380.00	2750.20	10.52	0.38	1.73

^aStandard uncertainties u are $u(T) = 0.03$ K. The values of $u(x_1)$ and $u(P)$ are given in the table.

values for each mixture was used as the repeatability value in the calculation of overall combined uncertainty for each point in that mixture.

As previously described in the Experimental section, great care was taken to maintain a minimal vapor space at the top of the equilibrium cell during measurements. This practice allowed for the assumption that the line leading out of the thermostatted system to the pressure transducer (which was located approximately 30 cm above the cell) was filled with vapor. If this were the case the head pressure correction would be negligible; however, if surface tension caused much of the line above the cell to the pressure transducer to be filled with liquid as opposed to condensing back into the cell, there would be a head pressure contribution to the measured bubble-point pressure. The pressure transducer was maintained at 313 K during measurements. Thus for temperatures below this, it was assumed the head pressure had no contribution to the

Table 6. Measured Bubble-Point Pressures for the System R-E347MCC + Pentane at Temperature T , Pressure P , and Liquid Mole Fraction x^a

$x_1 = 0.348 \pm 0.004$				
T/K	P/kPa	$u(P)/kPa$	$(u(P)/P) \cdot 100$	$(1 - P_{EOS}/P_{exp}) \cdot 100$
290.00	73.77	3.98	5.40	4.11
300.00	105.13	4.08	3.88	2.03
310.00	146.27	4.18	2.85	0.43
320.00	201.14	6.83	3.40	0.21
320.00	202.65	6.83	3.37	0.95
320.00	202.71	6.83	3.37	0.98
330.00	272.38	6.90	2.53	0.72
340.00	359.11	6.97	1.94	0.59
350.00	465.46	7.04	1.51	0.56
360.00	593.87	7.12	1.20	0.56
360.00	593.82	7.12	1.20	0.55
370.00	745.87	7.22	0.97	0.42
380.00	926.33	7.40	0.80	0.45
$x_1 = 0.667 \pm 0.007$				
T/K	P/kPa	$u(P)/kPa$	$(u(P)/P) \cdot 100$	$(1 - P_{EOS}/P_{exp}) \cdot 100$
269.96	31.92	3.68	11.53	5.84
280.07	49.27	3.73	7.58	4.03
290.00	73.11	3.79	5.18	2.69
290.00	74.92	3.79	5.06	5.04
299.98	106.55	3.85	3.61	2.57
300.08	104.29	3.84	3.69	0.09
300.00	105.10	3.84	3.66	1.15
310.00	145.44	3.90	2.68	-1.33
310.09	146.78	3.90	2.66	-0.72
320.00	200.18	5.12	2.56	-1.79
330.00	271.37	5.17	1.91	-1.47
330.00	271.92	5.17	1.90	-1.27
340.00	358.65	5.23	1.46	-1.67
339.97	359.92	5.23	1.45	-1.23
350.03	469.24	5.30	1.13	-1.13
360.02	600.52	5.36	0.89	-1.09
370.00	755.04	5.46	0.72	-1.36

^aStandard uncertainties u are $u(T) = 0.03$ K. The values of $u(x_1)$ and $u(P)$ are given in the table.

measurement. At temperatures of 320 K and above, the head pressure was calculated for each point and treated as an uncertainty in the calculation of the overall uncertainty in the reported bubble-point pressures. For the more dense samples, this correction resulted in a significant increase in the estimated overall uncertainty.

The overall combined uncertainty for each point was calculated by taking the root sum of squares of the pressure equivalents of the temperature and composition uncertainties, the uncertainty in pressure, the measurement repeatability, and head pressure corrections. This number was multiplied by two ($k = 2$) and is reported as an uncertainty in pressure as well as a percent uncertainty for each bubble point.

5. RESULTS AND CORRELATION OF DATA

The measured bubble points for the eight binary mixtures (two compositions for each pair) are reported in Tables 1 through 8. The data were correlated with an excess Helmholtz energy model. The Helmholtz energy is a fundamental property with independent variables of density and temperature, from which all other thermodynamic properties can be calculated as

Table 7. Measured Bubble-Point Pressures for the System R-E347MCC (1) + Novac 649 (2) at Temperature T , Pressure P , and Liquid Mole Fraction x^a

$x_1 = 0.308 \pm 0.004$				
T/K	P/kPa	$u(P)/kPa$	$(u(P)/P) \cdot 100$	$(1 - P_{EOS}/P_{exp}) \cdot 100$
290.00	41.69	4.53	10.86	6.30
300.00	59.12	4.55	7.70	0.19
300.00	60.24	4.55	7.56	2.05
310.00	86.50	4.58	5.29	0.35
310.00	86.36	4.58	5.30	0.20
320.00	123.22	10.12	8.21	0.76
320.00	121.67	10.12	8.32	-0.50
330.00	171.75	10.14	5.90	1.57
330.00	168.96	10.14	6.00	-0.05
340.00	232.36	10.15	4.37	1.67
340.00	231.44	10.15	4.39	1.29
350.00	308.13	10.17	3.30	1.78
350.00	307.83	10.17	3.30	1.69
360.00	401.36	10.18	2.54	1.87
360.00	401.00	10.18	2.54	1.78
370.00	514.45	10.20	1.98	1.92
380.00	650.26	10.23	1.57	1.97
$x_1 = 0.701 \pm 0.002$				
T/K	P/kPa	$u(P)/kPa$	$(u(P)/P) \cdot 100$	$(1 - P_{EOS}/P_{exp}) \cdot 100$
290.00	54.52	3.10	5.68	11.80
300.00	77.69	3.18	4.10	6.90
310.00	107.28	3.27	3.05	1.89
310.00	107.39	3.27	3.05	1.99
320.00	151.44	9.19	6.07	1.78
330.00	207.09	9.22	4.45	1.05
340.00	277.58	9.26	3.34	0.58
340.00	277.54	9.26	3.34	0.57
350.00	365.51	9.30	2.54	0.34
360.00	473.25	9.34	1.97	0.17
370.00	603.39	9.39	1.56	0.04
380.00	758.84	9.46	1.25	-0.07

^aStandard uncertainties u are $u(T) = 0.03$ K. The values of $u(x_1)$ and $u(P)$ are given in the table.

derivatives. As discussed in detail in Lemmon et al.,⁸ the Helmholtz energy for pure fluids is calculated as the sum of the contributions from the ideal gas and from the residual (or real gas) portions of the fluid. The model uses dimensionless values of density and temperature for the independent parameters, where the critical point properties are used as the reducing values. The equations of state for the pure fluids required to implement this model are given by Bucker and Wagner⁹ for butane, Span and Wagner¹⁰ for pentane, Lemmon and Span¹¹ for R-141b and R-245fa, McLinden et al.¹² for R-1234ze(E), Zhou et al.¹ for R-E347mcc, Wu et al.¹³ for DME, and McLinden et al.¹⁴ for Novac 649.

Mixtures are modeled by summing the mole fraction contributions from the pure fluid equations of state and a contribution from mixing (often called the departure function). The reducing parameters for the mixture are not the critical point of the mixture, but empirical equations with adjustable parameters outlined by Kunz and Wagner.¹⁵ These equations use the critical points of the pure fluids and up to four additional optimized parameters for each binary mixture. Two of the parameters are used to define the reducing values for temperature and two for the reducing values of density. The

Table 8. Measured Bubble-Point Pressures for the System Novac 649 (1) + Pentane (2) at Temperature T , Pressure P , and Liquid Mole Fraction x^a

$x_1 = 0.178 \pm 0.003$				
T/K	P/kPa	$u(P)/kPa$	$(u(P)/P) \cdot 100$	$(1 - P_{EOS}/P_{exp}) \cdot 100$
290.04	65.37	3.54	5.41	2.37
300.04	95.01	3.63	3.82	2.63
310.04	130.60	3.73	2.86	0.19
320.00	180.92	6.39	3.53	1.09
330.06	245.30	6.45	2.63	1.77
329.96	244.62	6.45	2.64	1.77
340.02	324.15	6.52	2.01	2.11
349.91	418.66	6.59	1.57	2.10
349.96	418.79	6.59	1.57	2.01
359.97	534.66	6.66	1.25	2.09
369.91	671.37	6.74	1.00	2.07
$x_1 = 0.406 \pm 0.006$				
T/K	P/kPa	$u(P)/kPa$	$(u(P)/P) \cdot 100$	$(1 - P_{EOS}/P_{exp}) \cdot 100$
300.01	93.35	2.44	2.61	-2.76
300.06	93.89	2.44	2.60	-2.36
310.03	134.11	2.50	1.86	-1.11
310.01	134.09	2.50	1.86	-1.06
319.99	184.4	7.44	4.04	-1.17
330.02	249.02	7.06	2.84	-1.01
340.01	329.6	7.09	2.15	-0.77
350.04	428.85	7.12	1.66	-0.59
360	547.38	7.16	1.31	-0.60
360.02	547.6	7.16	1.31	-0.61
369.91	688.71	7.20	1.04	-0.56

^aStandard uncertainties u are $u(T) = 0.03$ K. The values of $u(x_1)$ and $u(P)$ are given in the table.

data reported in this work are the only data available for these mixtures. As such, they do not constitute a large enough collection to use the departure function or the reduced density contributions to the equation.

All of the equations required to calculate thermodynamic properties of the mixtures studied in this work can be found in the publication of Kunz and Wagner.¹⁵ Only the equations for the reducing parameters will be repeated here. These equations are

$$T_r(x) = \sum_{i=1}^N \sum_{j=1}^N x_i x_j \beta_{T,ij} \gamma_{T,ij} \frac{x_i + x_j}{\beta_{T,ij} x_i + x_j} (T_{c,i} \cdot T_{c,j})^{0.5} \quad (1)$$

$$\frac{1}{\rho_r(x)} = \sum_{i=1}^N \sum_{j=1}^N x_i x_j \frac{1}{8} \left(\frac{1}{\rho_{c,i}^{1/3}} + \frac{1}{\rho_{c,j}^{1/3}} \right)^3 \quad (2)$$

The adjustable parameters in the reducing values for density have been removed from eq 2 because they were not used in this work. In these equations, N is the number of components in the mixture, $T_{c,i}$ is the critical temperature of component i , $\rho_{c,i}$ is the critical density of component i , x_i is the molar composition of component i , and T_r and ρ_r are the reducing values used in the equations of Kunz and Wagner.¹⁵ The symbols $\beta_{T,ij}$ and $\gamma_{T,ij}$ are adjustable parameters used to optimize the model to the experimental data. The values obtained from fitting the measured data of this work are given in Table 9. Calculated values of the bubble-point pressure at 300 K are

Table 9. Mixture Parameters for Helmholtz Energy Models

mixture	$\beta_{T,ij}$	$\gamma_{T,ij}$	pressure (MPa) at 300 K ^a
butane/R-245fa	1.02	0.904	0.32389
pentane/R-141b	1.0	0.977	0.087803
pentane/R-245fa	1.0	0.90	0.18649
pentane/R-1234ze(E)	0.993	0.937	0.39648
pentane/DME	0.962	0.999	0.39206
pentane/RE347mcc	1.0	0.928	0.10604
Novec 649/RE347mcc	0.989	0.98	0.067884
pentane/Novec 649	1.0	0.894	0.095763

^aCalculated at a 0.50/0.50 mole fraction composition for each mixture. Additional digits are given for use in algorithm verification only.

given to validate calculations from independent sources using the reducing parameters and equations of state given above.

Figure 2 shows the percent deviations between the measured bubble-point data presented here and the Helmholtz energy models with the fitted parameters from Table 9. Deviations for the mixtures R-E347MCC + Novec 649, R-E347mcc + pentane, Novec 649 + pentane, and DME + pentane are

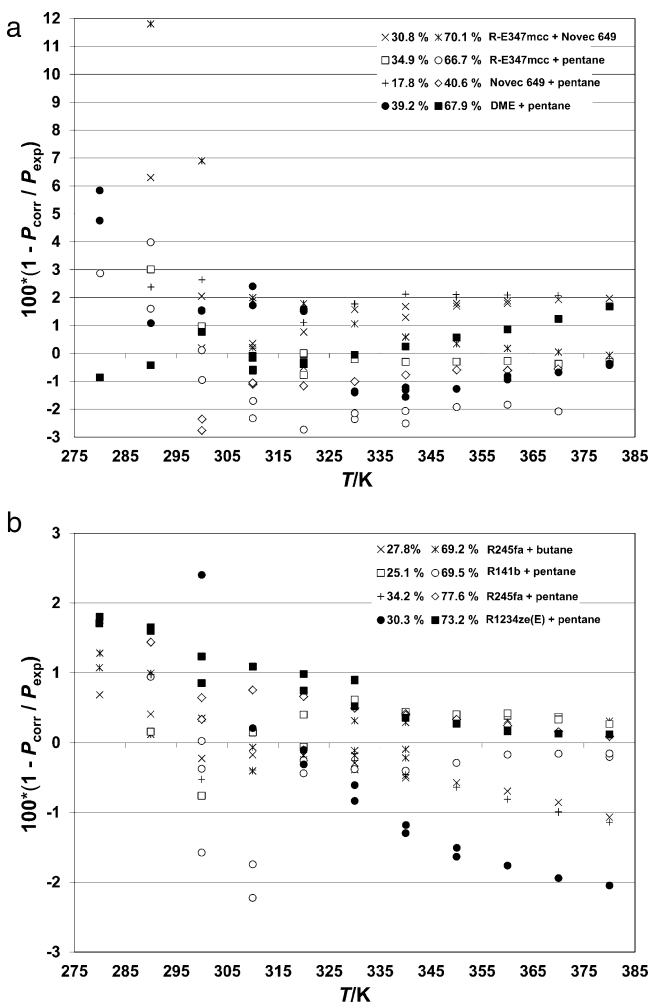


Figure 2. (a) Deviations from the Helmholtz energy correlations for the mixtures R-E347MCC + Novec 649, R-E347MCC + pentane, Novec 649 + pentane, and DME + pentane as a function of temperature. (b) Deviations from the Helmholtz energy correlations for the mixtures R-245fa + butane, R-141b + pentane, R245fa + pentane, and R1234ze(E) + pentane as a function of temperature.

shown in Figure 2a, with the remaining mixture deviations shown in Figure 2b. The deviation of 11.8 % shown in Figure 2a is for the R-E347mcc + Novec 649 mixture (70.1 mol % R-E347MCC) at 290 K. The rest of the mixture deviations fall within $\pm 7\%$; the majority of them are within $\pm 2\%$, and the average absolute deviation (AAD) is 1.1 %. Deviations from the respective equations are listed numerically in Tables 1 to 8.

Care was taken during fitting to use the least number of parameters possible to fit the bubble-point pressure to avoid overfitting. The available parameters in the reduced density equation (which were removed from eq 2) could have been used to decrease the deviations in bubble-point pressures; however, without mixture density data at a variety of temperatures and compositions, the additional parameters would have likely increased the error in density. (Without the availability of measurements on the densities for these mixtures, the uncertainty in density is unknown.) Thus, higher errors are seen in Figure 2 than would have been obtained if density measurements had been available. Further experimental work will enable the use of more fitted parameters to decrease the uncertainty in calculated properties.

6. DISCUSSION AND CONCLUSIONS

A total of 237 bubble-point pressures were measured for eight binary mixtures (two compositions for each mixture) at temperatures from 270 K to 380 K. The bubble-point pressures of the 16 sample mixtures ranged from 31 kPa to 2800 kPa. Each mixture was correlated with a Helmholtz energy model, and the majority of the data were fitted within $\pm 2\%$. Approximately 86 % (203) of the bubble points were fitted within their combined overall experimental uncertainty. The largest deviations (all of those above 3 %) occur at temperatures of 300 K and below. The data on mixtures containing R-E347 mmc (with large deviations) have very low bubble-point pressures at those temperatures, less than 80 kPa. Thus, even small uncertainties, for example, that of the pressure reading (0.7 kPa) could produce significant deviations. The cause of the large deviations of the DME + pentane mixture at 280 K is unclear. It might be due to difficulty in accurately modeling the nonideal behavior of this mixture as it is a polar/nonpolar pair. This, however, would not necessarily explain why the large deviations occur at the lowest temperatures and not over the entire temperature range or why they occur only for the pentane-rich composition of this mixture.

Utilizing mixtures as working fluids in Organic Rankine Cycles creates countless options to create the optimal working fluid for a given set of equipment and operating conditions. Siddiqi and Atakan^{16,17} as well as others^{2,18–20} have explored the potential of mixtures through calculations based on theoretical conditions. In general, these works lend support to the promise of increased efficiency of ORC systems through the use of mixtures as working fluids; however, because many potential mixtures include components for which little or no experimental thermodynamic mixture data exist, a gap between calculations based on theory and real world performance may exist.

The mixtures studied in this work were chosen to explore their possibility as Organic Rankine Cycle working fluids that would have more favorable thermodynamic properties as well as a lower global warming potential (GWP) than those of existing fluids. Many of the mixtures included polar + nonpolar component pairs and/or components with significant differences in their molecular size and shape. These types of mixtures

can be difficult to model accurately (especially when the data are sparse) because their properties tend to deviate from ideal thermodynamic mixing,²¹ and thus, experimental data are needed.

The measurement method followed in this work was designed to eliminate the need for mixture composition analysis as mixtures were prepared gravimetrically and measurements were carried out to support the assumption that the liquid composition of the sample mixture studied was that of the bulk composition of the prepared sample. This approach is advantageous because a high degree of uncertainty is associated with composition analyses of mixtures regardless of whether it is conducted in situ or otherwise. Thus, the sample preparation and measurement methods used in this study have simplified the measurement process and eliminated a source of uncertainty. Results indicate that we have measured bubble-point pressures of binary mixtures with good repeatability and at a level of uncertainty that facilitates the formulation of equations of state with uncertainties small enough to aid in the design of more efficient systems for energy production.

AUTHOR INFORMATION

Corresponding Author

*E-mail: stephanie.outcalt@nist.gov.

Notes

The authors declare no competing financial interest.

ACKNOWLEDGMENTS

We thank Drs. Tara Lovestead, Bret Windom, and Jason Widgren for providing analysis of the pure fluids used to prepare the binary mixtures studied in this work. This material is based upon work supported by the Department of Energy [Geothermal Technologies Program] under award DE-EE0002770 [Tailored Working Fluids for Enhanced Geothermal Power Plants] to the United Technologies Research Center (PI: Dr. Ahmad M. Mahmoud). This paper was prepared as an account of work sponsored by an agency of the United States government. Neither the United States government nor any agency thereof, nor any of their employees, makes any warranty, express or implied, or assumes any legal liability or responsibility for the accuracy, completeness, or usefulness of any information, apparatus, process, or process disclosed, or represents that its use would infringe privately owned rights. Reference herein to any specific commercial product, process, or service by trade name, trademark, manufacturer, or otherwise does not necessarily constitute or imply its endorsement, recommendation, or favoring by the United States government or any agency thereof. The views and opinions of authors expressed herein do not necessarily reflect those of the United States government or any agencies thereof. The authors are grateful for the support of the Department of Energy (DOE).

REFERENCES

- (1) Zhou, Y.; Lemmon, E. W.; Mahmoud, A. M. Equations of state for RE245cb2, RE347mcc, RE245fa2, and R1216. To be submitted to *J. Phys. Chem. Ref. Data*, **2013**.
- (2) Stijepovic, M.; Linke, P.; Albatrni, H.; Kanis, R.; Nisa, U.; Hamza, H.; Shiraz, I.; El Meragawi, S. *Qatar Foundation Annual Research Forum*, Doha, Qatar, 2011 EG01.

- (3) Stein, S. E. *NIST/EPA/NIH Mass Spectral Library with Search Program, NIST Standard Reference Database 1A*; NIST: Gaithersburg, MD, 2005.

- (4) Bruno, T. J.; Svoronos, P. D. N. *CRC Handbook of Basic Tables for Chemical Analysis*, 3rd ed.; Taylor and Francis, CRC Press: Boca Raton, FL, 2011.

- (5) Harris, G. L.; Torres, J. A. *Selected laboratory and measurement practices and procedures to support basic mass calibrations*, NIST-IR 6969; NIST: Boulder, CO, 2003.

- (6) Outcalt, S. L.; Lee, B. C. A Small-Volume Apparatus for the Measurement of Phase Equilibria. *J. Res. Natl. Inst. Stand. Technol.* **2004**, *109*, 525–531.

- (7) Taylor, B. N.; Kuyatt, C. E. *Guidelines for Evaluating and Expressing the Uncertainty of NIST Measurement Results*, NIST Technical Note 1297; U.S. Department of Commerce: Washington, DC, 1994.

- (8) Lemmon, E. W.; McLinden, M. O.; Wagner, W. Thermodynamic Properties of Propane. III. A Reference Equation of State for Temperatures from the Melting Line to 650 K and Pressures up to 1000 MPa. *J. Chem. Eng. Data* **2009**, *54*, 3141–3180.

- (9) Bücker, D.; Wagner, W. Reference Equations of State for the Thermodynamic Properties of Fluid Phase n-Butane and Isobutane. *J. Phys. Chem. Ref. Data* **2006**, *35*, 929–1019.

- (10) Span, R. W.; Wagner, W. Equations of State for Technical Applications. II. Results for Nonpolar Fluids. *Int. J. Thermophys.* **2003**, *24*, 41–109.

- (11) Lemmon, E. W.; Span, R. Short Fundamental Equations of State for 20 Industrial Fluids. *J. Chem. Eng. Data* **2006**, *51*, 785–850.

- (12) McLinden, M. O.; Thol, M.; Lemmon, E. W. Thermodynamic Properties of Trans-1,3,3,3-Tetrafluoropropene [R1234ze(E)]: Measurements of Density and Vapor Pressure and a Comprehensive Equation of State. *Proc. Int. Refrig. Air Conditioning Conf. Purdue*, July 12–15, **2010**.

- (13) Wu, J.; Zhou, Y.; Lemmon, E. W. An Equation of State for the Thermodynamic Properties of Dimethyl Ether. *J. Phys. Chem. Ref. Data* **2011**, *40*, 1–16.

- (14) McLinden, M. O.; Perkins, R. A.; Lemmon, E. W.; Fortin, T. Thermodynamic Properties of 1,1,1,2,2,4,5,5,5-Nonafluoro-4-(Trifluoromethyl)-3-Pentanone. To be submitted to *J. Chem. Eng. Data*, **2012**.

- (15) Kunz, O.; Wagner, W. The GERG-2008 Wide-Range Equation of State for Natural Gases and Other Mixtures: An Expansion of GERG-2004. *J. Chem. Eng. Data* **2012**, *57*, 3032–3091.

- (16) Siddiqi, M. A.; Atakan, B. Investigation of the Criteria for Fluid Selection in Rankine Cycles for Waste Heat Recovery. *Int. J. Thermodyn.* **2011**, *14*, 117–123.

- (17) Siddiqi, M. A.; Atakan, B. *The 25th International Conference on Efficiency, Cost, Optimization, Simulation and Environmental Impact of Energy Systems*, Perugia, Italy, June 26–29, **2012**; 246–241–246–217.

- (18) Angelino, G.; Di Paliano, P. C. Multi-component working fluids for organic Rankine cycles (ORCs). *Energy* **1998**, *23*, 449–463.

- (19) Chen, H.; Goswami, D. Y.; Rahman, M. M.; Stefanakos, E. K. A supercritical Rankine cycle using zeotropic mixture working fluids for the conversion of low-grade heat into power. *Energy* **2011**, *36*, 549–555.

- (20) Maizza, V.; Maizza, A. Unconventional working fluids in organic Rankine-cycles for waste energy recovery systems. *Appl. Therm. Eng.* **2001**, *21*, 381–390.

- (21) Outcalt, S. L.; Laesecke, A. Compressed-liquid densities of two highly polar + non-polar binary systems. *J. Mol. Liq.* **2012**, *173*, 91–102.